

The effect of density fluctuations in supercritical fluids: new science and technology for polymer thin films

Tadanori Koga^{a,*}, E. Akashige^a, A. Reinstein^b, M. Bronner^c, Y.-S. Seo^d, K. Shin^e,
M.H. Rafailovich^a, J.C. Sokolov^a, B. Chu^f, S.K. Satija^d

^aDepartment of Materials Science & Engineering, State University of New York at Stony Brook, Stony Brook, NY 11794-2275, USA

^bRambam Mesivta High School, Lawrence, NY 11559, USA

^cYale University, New Haven, CT 06520, USA

^dCenter for Neutron Research, National Institute of Standards and Technology, Gaithersburg, Maryland 20899, USA

^eDepartment of Materials Science and Engineering, K-JIST, Kwang-ju 500-712, Korea

^fDepartment of Chemistry, State University of New York at Stony Brook, Stony Brook, NY 11794-3400, USA

Abstract

Supercritical carbon dioxide (scCO₂) is being used increasingly as a green solvent in polymer processing. However, the major disadvantage thus far is that only a limited class of polymers, such as fluorinated or silicone-based polymers, can be dissolved in scCO₂. Here we show that large density fluctuations in scCO₂ can significantly enhance the solubility of scCO₂ with polymer thin films even when the bulk polymers have very poor miscibility with scCO₂. In addition, by utilizing quick solvent evaporation of CO₂, we could preserve the swollen structures, resulting in low-density polymer thin films where nanometer-scale porosity was significantly introduced. The use of the low-density polymer thin films could allow us to develop a new gas membrane that could selectively permit a large flow of small molecule gases, such as O₂ and CO₂, while completely blocking out larger gases or particulates.

© 2004 Elsevier B.V. All rights reserved.

PACS: 61.41.+e; 61.25.Hq

Keywords: Supercritical fluids; Density fluctuations; Polymer thin films; Swelling; Gas membrane; Low-density polymer films

1. Introduction

At temperatures and pressures above the critical point values, a one-component fluid can have density and solvent properties approaching those of the corresponding liquid. Fluids in this regime

*Corresponding author. Tel.: +1 631 632 3209; fax: +1 631 632 5764.

E-mail address: tkoga@notes.cc.sunysb.edu (T. Koga).

are defined as “supercritical fluids” (SCFs) (Fig. 1). At liquidlike densities SCFs exhibit a gaslike low viscosity and high diffusion rate. In addition, by varying temperature and pressure, one can control the solute–solvent interactions in SCFs. In particular, much attention has been focused on supercritical carbon dioxide (scCO₂) since scCO₂ is an environmentally clean solvent having the mild critical point value ($T_c = 31.3^\circ\text{C}$ and $P_c = 7.38\text{ MPa}$). ScCO₂ is being used increasingly as a regeneration solvent in polymer processing, polymer synthesis, reactor cleanup, and preparation of pharmaceutical products [1]. However, the major disadvantage thus far is that only a limited class of polymers, such as highly fluorinated or silicone-based polymers, can be dissolved in scCO₂ under moderate conditions ($T < 100^\circ\text{C}$, and $P < 50\text{ MPa}$) [1–4]. Therefore, it is crucial to develop a new concept for improving the solubility of target materials with scCO₂.

In this paper, we first review our new finding: density fluctuations in scCO₂ near the critical point can drastically enhance the swelling of polymer thin films even when the bulk polymers have the very poor miscibility with scCO₂. The key technique is neutron reflectivity (NR), which is an ideal tool to determine the in situ thickness, composition, and interfacial structures of polymer thin films immersed in fluids or gases, under high

pressure. The NR studies clarify that a wide variety of polymer thin films can swell as much as 30–60% in scCO₂ along the “density fluctuation ridge” [5,6] that defines the maximum density fluctuation amplitude of CO₂ in the P – T phase diagram (Fig. 1). The ridge separates into the more liquidlike and more gaslike regions in the supercritical region and is a general feature for substances [7,8].

Furthermore, we find that the in situ film quality, i.e., density, roughness and film thickness, can be frozen by quick evaporation of CO₂ [9]. This process vitrifies the polymer without formation of micron-sized voids that are known to form in the bulk when scCO₂ is forced under high pressures into polymers with which it is immiscible [10,11]. Here, we show that the frozen thin films where molecular scale porosity is significantly introduced [12] play an important role as a highly permeable gas membrane for gas filtration.

2. Neutron reflectivity

In order to perform reflectivity measurements under compressed gases or liquids, there are several experimental difficulties. Especially, delivering probe beams, such as X-ray and neutron into high-pressure vessels is the most important issue due to a large absorption of the compressed gases for the radiation beams. For instance, the linear absorption coefficient (μ) of CO₂ with density (ρ_{co}) of 0.468 g/cm^3 , which corresponds to the critical density, is estimated to be 2.71 cm^{-1} with a X-ray wavelength of 1.3 \AA . The transmittance beam through a path-length of t , $I(t) = e^{-\mu t}$, is almost absorbed when $t > 2\text{ cm}$. Although similar absorption of neutron beams occurs in compressed CO₂, it is possible to overcome this difficulty by utilizing the large penetration depth inherent with neutrons: incident and reflected beams can pass through a Si substrate without contact CO₂ [6].

The specular NR measurements were performed on the NG-7 reflection spectrometer at National Institute of Standards and Technology. The details of the high-pressure cell and data analysis have been described elsewhere [6].

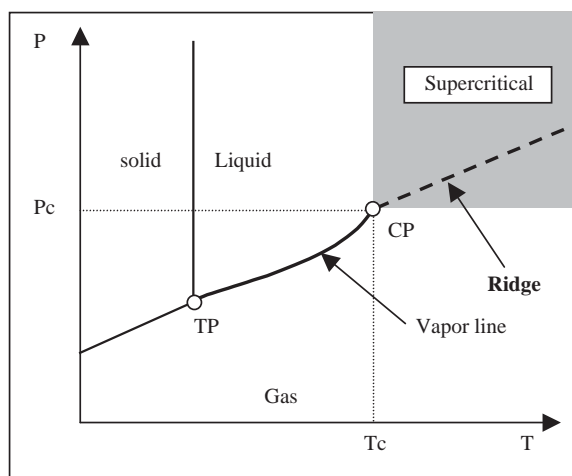
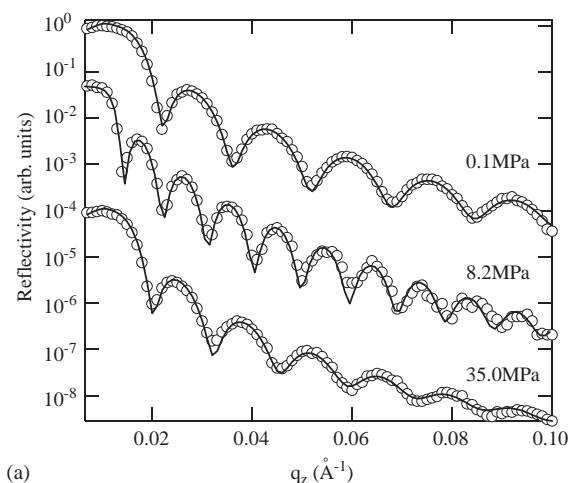


Fig. 1. Schematic phase diagram of CO₂. Supercritical fluid state and triple point are denoted as SCF and TP, respectively.

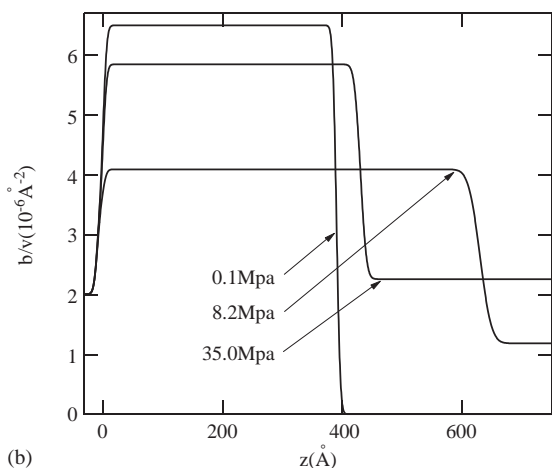
3. Results and discussion

3.1. Anomalous swelling of polymer thin films in $sc\text{CO}_2$

Fig. 2(a) shows representative NR data for a deuterated styrene-random-butadiene copolymer (d-SBR) thin film at three different pressures and $T = 36^\circ\text{C}$; the reflected scattering intensity is plotted as a function of the momentum transfer normal to the surface, $q_z = 4\pi \sin \theta / \lambda$, where θ is



(a)



(b)

Fig. 2. (a) Representative reflectivity data for d-SBR films at $T = 36^\circ\text{C}$. Consecutive reflectivities have been offset from each other for clarity. Solid lines represent reflectivity calculated from the corresponding d-SBR concentration profiles shown in (b).

the glancing angle of incidence and λ is a wavelength of neutron beams. The solid lines correspond to the best-fits to the data based on the scattering length density (SLD) profiles shown in Fig. 2(b). From the figure we can see that the good fits can be obtained with uniform concentrations of CO_2 into the polymer layer and no preferential adsorption of either CO_2 or polymer occurs at the Si substrate. The thickness of the layer, which is initially 385 \AA thick, increased drastically to 620 \AA near the critical pressure ($P = 8.2 \text{ MPa}$) and then decreased again to 423 \AA upon compression up to $P = 35.0 \text{ MPa}$. It was found that the swelling behavior was an equilibrium quantity that was solely a function of the CO_2 pressure and temperature [5,13].

Fig. 3(a) summarizes the swelling behavior of the d-SBR thin films. The linear dilation (S_f) was calculated from the equation $S_f = (L - L_0)/L_0$, where L and L_0 are the measured thickness of the swollen and unswollen polymer thin films, respectively. From the figure we can see that each swelling isotherm shows a peak near the critical pressure. Especially at $T > T_c$, as the temperature approached to T_c , the peak profile became sharper accompanying a position shift to the lower pressure. When the pressure increased well into the liquid or supercritical region ($P \approx 15 \text{ MPa}$), the film collapsed and only a small dilation of approximately 0.1 appeared for all isothermal conditions studied.

Isothermal swelling data of a bulk SBR sample ($M_w = 35,000$, $M_w/M_n = 1.8$, $\phi_{\text{PS}} = 24\%$, 8 mm in thick, Goodyear Co.) determined by a cathetometer is also plotted (shown by filled circles) in Fig. 3(a) at $T = 36^\circ\text{C}$. To compare the swelling between the thin and bulk films, we assumed that the swelling of the thin films was uniaxial [14,15], while that of the bulk (S_b) was isotropic, i.e., $S_b = ((L - L_0)/L_0)^3$. From the figure we can see that the bulk result is similar to those reported for other polymers [16–24]: the rate of the dilation is maximal near the critical pressure, and a plateau, with no maxima, in the swelling at a value of 10% occurs. Hence the bulk swelling is related to the monotonic increase in the miscibility of the polymer with CO_2 above T_c [5]. Since only the rate of miscibility, rather than the absolute value,

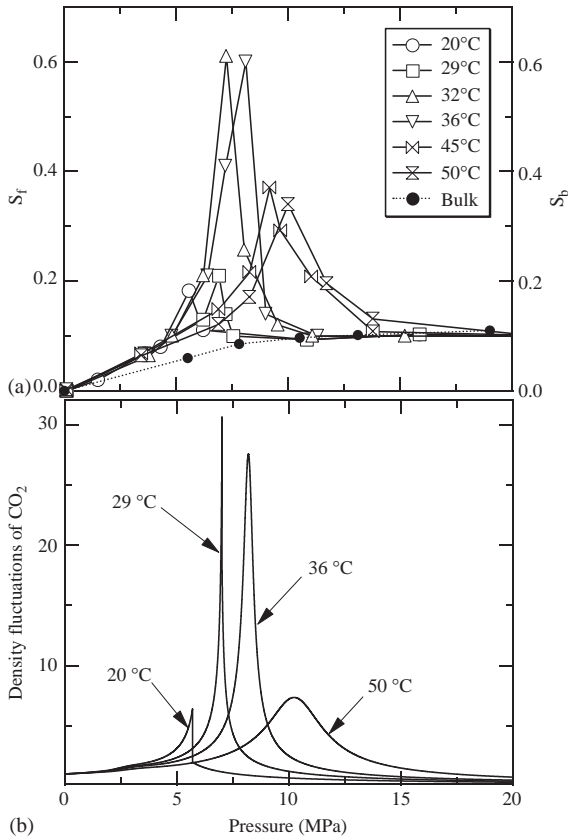


Fig. 3. (a) Pressure dependence of S_f for d-SBR in CO_2 . S_b for bulk SBR at $T = 36^\circ\text{C}$ is also shown by filled circles. (b) Calculated density fluctuations of CO_2 based on Eq. (1).

is maximal near P_c , this does not explain the peak observed in the dilation curves of thin films.

What is the driving force for this anomalous dilation? The key was the scattering intensity from CO_2 , i.e., the density fluctuations, as the background scattering for the NR data [6]. As a result, we found that the pressure dependence of the integrated scattering intensity also showed a peak at the same position (pressure) where the anomalous swelling occurred [5]. In order to further explore the relationship between the density fluctuations in CO_2 and anomalous dilation, we calculated the density fluctuations, $\langle(\Delta N)^2\rangle/\langle N\rangle$, using the thermodynamic relationship:

$$\langle(\Delta N)^2\rangle/\langle N\rangle = (N/V)\kappa_T k_B T, \quad (1)$$

where N is the number of molecules in the corresponding volume V , and k_B is the Boltzmann constant. The isothermal compressibility κ_T was obtained by using the equation of state derived by Huang et al. [25]. Fig. 3(b) shows the calculated density fluctuations at the four different isothermal conditions as a function of pressure. Each peak position in the curves forms the ridge in the P - T phase diagram shown in Fig. 1. Comparison of the experimental data shown in Fig. 3(a) with the calculated density fluctuations in Fig. 3(b) leads to an important conclusion that the anomalous dilation observed is strongly correlated to the density fluctuations in CO_2 . Furthermore, we found that the dilation curves under the two isobaric conditions ($P = 7.9$ and 10.8 MPa) could again be directly superimposed on the density fluctuation curves, as in the case of the isothermal curves [5]. We can therefore conclude that the dilation is an equilibrium phenomenon, which is associated only with $\langle(\Delta N)^2\rangle/\langle N\rangle$, and independent of the direction of approach to the ridge. This finding is, to the best of our knowledge, the first time to demonstrate that the density fluctuations can improve and control the solubility of scCO_2 in the polymer thin films. Since the large density fluctuations in scCO_2 can be achieved even near the room temperature, the effect is very important for polymer processing in which high temperature is typically required.

Here we summarize the further characteristics of the anomalous swelling of polymer thin films along the density fluctuation ridge:

- (1) The anomalous dilation is an universal phenomenon regardless of a choice of polymers. In addition, it is found that the dilation at the ridge appears to be more a function of the elasticity of the polymer than the solubility parameter [6];
- (2) The anomalous dilation can be collapsed on an universal curve when the film thickness is scaled by R_g , where R_g is the radius of polymer gyration, and is a surface effect that occurs within the $10R_g$ thickness at the polymer/ CO_2 interface [5].

We also studied the swelling behavior of deuterated polystyrene (d-PS) brushes, where chain ends of which are chemically grafted to a solid surface [26]. The NR measurements clearly demonstrated that the swelling behavior of the d-PS brushes was identical to that of the non-tethered d-PS thin film, including the anomalous swelling region near the ridge. Furthermore, the density profiles of the d-PS brushes could be approximated by a simple step function within the entire pressure ranges used, indicating that the solvent quality of scCO₂ was still poor for the d-PS brush even at the ridge.

3.2. Highly gas permeable membrane using low-density polymer thin films

Over the past several years, the demand for safer and more effective gas masks has increased dramatically with the threat of biological and chemical terrorism, as well as with the outbreak of SARS and other extremely contagious viruses. Gas masks are currently produced using “non-woven” fiber technology, where fibers are compacted to produce a porous filter. This technique can yield filters with very small pores. On the one hand, this technology is very effective in blocking pathogens such as anthrax, but on the other, these filters can be very uncomfortable since they also restrict the flow of air, and if they are frequently removed, they are not effective. Thus, the ideal gas mask would be one that allow unrestricted airflow while selectively blocking out airborne pathogens. Here we show that the low-density polymer thin films created by the scCO₂ processing have great potential to develop such a membrane.

Polymer used in this study was PS ($M_w = 6.5 \times 10^5$, $M_w/M_n = 1.05$, Polymer Lab.). The film thickness of 1500 Å was spun cast onto a glass slide. The sample preparation for oxygen gas permeability experiments is as follows: (i) the spun-cast film was placed in the high pressure chamber, (ii) immersed in scCO₂ at given pressures and $T = 36^\circ\text{C}$ for the annealing time of 2 h, (iii) quickly depressurized to the atmospheric pressure within 10 s, and (iv) floated onto deionized water and subsequently lifted onto a polished washer with the PS film covering an entire hole (a 5-mm

diameter). An oxygen gas detector and LabPro interface (Verner Software and Technology) were used for the real-time data collections. Since we utilized oxygen gas in the air, the atmosphere of the chamber, which was attached directly to the gas detector, was initially filled with nitrogen gas. The washer covered with the film was then placed onto the hole of the chamber and the oxygen gas flow through the film was monitored as a function of time. Fig. 4(a) shows the time dependence of the oxygen flow flux for the PS film before and after exposure to scCO₂ ($T = 36^\circ\text{C}$ and $P = 8.2\text{ MPa}$).

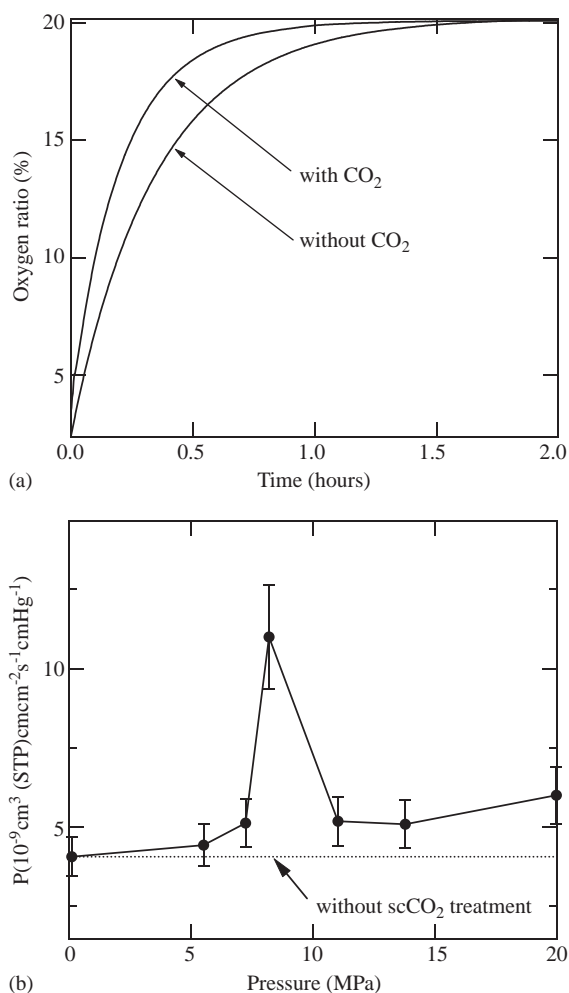


Fig. 4. (a) Oxygen flow flux vs. time for unexposed and exposed PS films. (b) Pressure dependence of intrinsic permeability coefficient is shown as a function of the film thickness.

From the figure we can see that the flow rate of the O_2 gas significantly increases after exposure to $scCO_2$. The time dependence of the gaseous flux (ϕ) could be approximated by a simple exponential function, i.e., the Fick's first law:

$$\phi = \alpha - \beta \exp(-t/\tau), \quad (2)$$

where α and β are constants, and τ is the time constant. τ is reversely proportional to the intrinsic permeability coefficient (P_i), i.e.,

$$\tau = VL_0/P_iA, \quad (3)$$

where V is the volume of the chamber, A is the surface area and L_0 is the initial film thickness. From the best fit to the data, the P_i value at the ridge was estimated to be 1.1×10^{-8} ($\text{cm}^3(\text{STP})\text{cm cm}^{-2}\text{s}^{-1}\text{cm Hg}^{-1}$), which is about three times larger than that of the unexposed film ($P_i = 4.0 \times 10^{-9}$ ($\text{cm}^3(\text{STP})\text{cm cm}^{-2}\text{s}^{-1}\text{cm Hg}^{-1}$)). Fig. 4(b) summarizes the effect of the CO_2 pressure on the P_i values at $T = 36^\circ\text{C}$. As in the case of the swelling behavior shown in Fig. 3(a), a sharp maximum appears at the density fluctuation ridge ($P = 8.2\text{ MPa}$). This indicates that molecular-level porosity is significantly introduced after the $scCO_2$ processing, resulting in a highly permeable membrane for O_2 gas. Interestingly, we found that the P_i value of the unexposed film was more than one order of magnitude larger than the bulk, $P_{\text{bulk}} = 2.5 \times 10^{-10}$ ($\text{cm}^3(\text{STP})\text{cm cm}^{-2}\text{s}^{-1}\text{cm Hg}^{-1}$). Further permeability experiments varying the film thickness of the PS thin films showed that the P_i values increased with decreasing the film thickness at $L_0 < 4000\text{ \AA}$ [27]. Hence, the low-density polymer thin films created by the $scCO_2$ processing could have great potential as an effective gas membrane. We are currently studying the gaseous flux of large molecules, such as SF_6 . Details will be published elsewhere [27].

4. Conclusion

We found that the large density fluctuations in $scCO_2$ significantly enhanced the solvent quality of $scCO_2$ for polymer thin films even when the bulk polymer has very poor miscibility with CO_2 . Since the poor miscibility of many interesting target

substances places a severe restriction on the widespread use of $scCO_2$ so far, this finding could facilitate a conceptual design and analysis of environmentally “green” chemical processing. In addition, by using the low-density polymer thin film created by the $scCO_2$ processing, we developed a new gas membrane that could permit a large flow of small molecule gases, such as O_2 and CO_2 . This membrane could be used in protective masks, making the masks effective yet relatively inexpensive for homeland security.

Acknowledgments

We thank J.F. Douglas for helpful discussions. Support of this work by the NSF-MRSEC is gratefully acknowledged.

References

- [1] M.A. McHugh, V. Krukonis, *Supercritical Fluids Extraction Principles and Practice*, Woburn, MA, 1994.
- [2] Z. Guan, J.M. DeSimone, *Macromolecules* 27 (1994) 5527.
- [3] D.A. Canelas, D.E. Betts, J.M. DeSimone, *Macromolecules* 29 (1996) 2818.
- [4] J.B. McClain, D. Londono, J.R. Combes, et al., *J. Am. Chem. Soc.* 118 (1996) 917.
- [5] T. Koga, Y.S. Seo, Y. Zhang, et al., *Phys. Rev. Lett.* 89 (2002) 125506.
- [6] T. Koga, Y.S. Seo, K. Shin, et al., *Macromolecules* 36 (2003) 5236.
- [7] K. Nishikawa, T. Morita, *Chem. Phys. Lett.* 316 (2000) 238.
- [8] T. Morita, K. Kusano, H. Ochiai, et al., *J. Chem. Phys.* 112 (2000) 4203.
- [9] T. Koga, Y.S. Seo, X. Hu, et al., *Europhys. Lett.* 60 (2002) 559.
- [10] K.A. Arora, A.J. Lesser, T.J. McCarthy, *Macromolecules* 31 (1998) 4614.
- [11] C.M. Stafford, T.P. Russell, T.J. McCarthy, *Macromolecules* 32 (1999) 7610.
- [12] T. Koga, Y.S. Seo, J. Jerome, et al., *Appl. Phys. Lett.* 83 (2003) 4309.
- [13] T. Koga, K. Shin, Y. Zhang, et al., *J. Phys. Soc. Japan* 70 (2001) 347.
- [14] D.F. Stamatiadis, M. Wessling, M. Sanopoulou, et al., *J. Membr. Sci.* 130 (1997) 75.
- [15] M.D. Sefcik, *J. Polym. Sci., Part B: Polym. Phys* 24 (1986) 935.
- [16] R.G. Wissinger, M.E. Paulaitis, *J. Poly. Sci. Polym. Phys. Ed.* 25 (1987) 2497.

- [17] Y. Zhang, K.K. Gangwani, R.M. Lemert, J. Supercritical Fluids 11 (1997) 115.
- [18] S.H. Chang, S.C. Park, J.J. Shim, J. Supercritical Fluids 13 (1998) 113.
- [19] S.K. Goel, E.J. Beckman, Polymer 34 (1993) 1410.
- [20] G.K. Fleming, W.J. Koros, Macromolecules 19 (1986) 2285.
- [21] J.J. Shim, K.P. Johnston, AIChE J 35 (1989) 1097.
- [22] B.J. Briscoe, S. Zakaria, J. Polym. Sci.: Part B 29 (1991) 989.
- [23] A. Garg, E. Gulari, W. Manke, Macromolecules 27 (1994) 5643.
- [24] J.R. Royer, J.M. DeSimone, S.A. Khan, Macromolecules 32 (1999) 8965.
- [25] F.H. Huang, M.H. Li, K.E. Starling, et al., J. Chem. Eng. Japan 18 (1985) 490.
- [26] T. Koga, Y. Ji, Y.S. Seo, et al., J. Polym. Sci., Part B: Polym. Phys 42 (2004) 3282.
- [27] T. Koga, E. Akashige, M.H. Rafailovich, et al., Manuscript in preparation.